International Journal of Minerals, Metallurgy and Materials
Volume 24, Number 6, June 2017, Page 701
DOI: 10.1007/s12613-017-1453-y

Low-frequency damping behavior of closed-cell Mg alloy foams reinforced with SiC particles

Wen-zhan Huang[1,2], *Hong-jie Luo*[1,2], *Yong-liang Mu*[1,2], *Hao Lin*[1,2], *and Hao Du*[3]

1) School of Metallurgy, Northeastern University, Shenyang 110819, China

2) Engineering Research Center of the Ministry of Education for Advanced Materials Preparation Technology, Shenyang 110819, China

3) Institute of Metal Research, Chinese Academy of Sciences, Shenyang 110016, China

(Received: 9 November 2016; revised: 14 December 2016; accepted: 15 December 2016)

Abstract: The damping properties of an Mg alloy foam and its composite foams were investigated using a dynamic mechanical thermal analyzer. The results show that the loss factors of both the Mg alloy and its composite foams are insensitive to temperature and loading frequency when the temperature is less than a critical temperature T_{crit}. However, it increases when the temperature exceeds the T_{crit} values, which are 200 and 250°C for the Mg alloy foam and the Mg alloy/SiC_p composite foams, respectively. The Mg alloy/SiC_p composite foams exhibit a higher damping capacity than the Mg alloy foam when the temperature is below 200°C. By contrast, the Mg alloy foam exhibits a better damping capacity when the temperature exceeds 250°C. The variation in the damping capacity is attributed to differences in the internal friction sources, such as the characteristics of the matrix material, abundant interfaces, and interfacial slipping caused by SiC particles, as well as to macrodefects in the Mg alloy and its composite foams.

Keywords: magnesium alloys; foams; silicon carbide; damping

1. Introduction

Undesirable mechanical vibration and wave propagation adversely affect the stability of rockets, satellites, vehicles, and scientific instruments [1–2]. Thus, high-damping materials are currently in great demand. Compared with commercial metal materials, composites of foamed metallic materials (FMM) often exhibit higher loss factors in combination with some other virtues, such as low density, high specific strength, good flame resistance, and the abilities to absorb energy, reduce vibration, and absorb sound [3–4].

Most previous researches on the damping properties of FMM have been focused on aluminum foam and its alloy foams. Liu *et al.* [5] and Han *et al.* [6] have studied the factors influencing the damping properties and the damping mechanism of Al foams in different frequency ranges. Pores and defects were considered as the main internal friction sources. Banhart *et al.* [7] studied the low-frequency damping properties of Al foams and found that the damping properties were closely related to the density. In the case of Al foams with 69% macro pore volume fractions, Wei *et al.* [8] found that the loss factor was related to temperature and amplitude. Wu *et al.* [9], Gui *et al.* [10], and Mu *et al.* [11] studied the damping properties of Al matrix composite foams reinforced with particles. Their results show that SiC and fly ash particles improve the damping property of metal matrix composite foams. For most porous materials, their damping property depends on five factors: temperature, frequency, strain amplitude, reinforcement particles, and pore-structure parameters such as density and cell size.

Mg possesses not only excellent damping properties but also some other advantages, such as a low density, suitable comprehensive mechanical properties, and good recovery [12]. Thus, Mg alloy foams, whose matrix density is approximately two-thirds that of aluminum foams, are more promising for use as ultra-light metal structural materials, multi-functional materials, and high-damping materials. A few recent investigations have been carried out on the com-

Corresponding author: Hong-jie Luo E-mail: neuhjluo@sina.com

pressive properties of pure Mg foam [13] and Mg alloy foams [14–16]. However, studies on the damping properties of Mg alloy foams remain limited.

In the present work, closed-cell Mg alloy foams were fabricated using $MgCO_3$ as the foaming agent and SiC particles as a stabilizing agent. The effects of temperature, frequency, and the size of SiC particles on the damping capacity of the closed-cell Mg alloy and its composite foams were investigated. The corresponding damping mechanism of the materials was discussed.

2. Experimental

2.1. Fabrication of Mg alloy/SiC_p composite foams

The raw material, i.e., Mg–12Al–3Ca alloy, was prepared by adding appropriate amounts of Al and Mg to the Mg–20Ca matrix alloy at 700°C. The matrix alloy was purchased from Shanxi Yinguang Magnesium Industry Group Co., Ltd. Closed-cell Mg alloy/SiC_p composite foams were fabricated using a melt foaming process, which comprised four steps. (1) The Mg–12Al–3Ca alloy was melted to 700°C in a stainless steel crucible placed in an electric resistance furnace. (2) The SiC particles used as a stabilizing agent (4wt%) were added into the melt at 580°C, which was subsequently stirred by a propeller at a rate of 2000 r/min for 300 s. (3) The $MgCO_3$ (100 μm) foaming agent was mixed with Al_2O_3 particles (100 μm) in a mass ratio of 1:1; the resulting mixture was added to the melt at 580°C, and the mixture was stirred at 1500 r/min for 120 s. In addition, Al_2O_3 particles were used as an assistant dispersive agent in this step. (4) After being held in the furnace at 620°C for 180 s, the crucible was taken out and cooled to room temperature by chilling water. The Mg alloy/SiC_p composite foams with densities in the range from 0.33 to 0.78 g/cm^3 and a cell size in the range from 0.6 to 0.8 mm were obtained through variation of the amount of the foaming agent added. SiC particles with the average sizes of 80 μm (denoted as "80-SiC_p") and 10 μm (denoted as "10-SiC_p") were selected as the stabilizing agent in the fabrication of Mg alloy/SiC_p composite foams. In the case of the Mg alloy foam, no SiC particles were added, whereas the other steps were the same as those used in the fabrication of Mg alloy/SiC_p composite foams.

2.2. Structure characterization

All foam specimens were cut to dimensions of 50 mm × 12 mm × 4 mm using an electric discharge machine. Each specimen's density was determined through its mass and physical dimensions, by which its porosity is defined as

$$P = 1 - \frac{\rho}{\rho_s} \quad (1)$$

where P is the porosity and ρ and ρ_s are the densities of the composite foams and the cell wall material, respectively.

Each specimen's microstructure was observed by scanning electron microscopy (SEM) on a microscope (Ultra Plus, Zeiss, Germany) equipped with an energy-dispersive X-ray spectroscopy (EDS) apparatus (X-Max, Oxford Instruments, England).

2.3. Damping tests

The damping behaviors of the foams were evaluated by dynamic mechanical thermal analysis (DMTA; DMA 242 E, NETZSCH-Gerätebau GmbH, Germany) using the three-point bending mode. During the ascending temperature cycle, the testing conditions were set as 0.5, 2.0, and 5.0 Hz in frequency and 5 μm in strain amplitude. The damping tests with different frequencies were carried out at the same amplitude at room temperature. The damping capacity is expressed as (characterized with) the loss factor β, which is determined by

$$\beta = E''/E' = \tan\alpha \quad (2)$$

where E'' and E' are the dynamic loss modulus and the storage modulus, respectively, and α is the delay angle of the dynamic displacement varying with the dynamic force.

3. Results and discussion

3.1. Morphology observation

Fig. 1 shows a typical cell structure of the Mg alloy foam (Fig. 1(a)) with a porosity of 80.7% and of the Mg alloy/SiC_p composite foams (Figs. 1(b) and 1(d)). In the case of the Mg alloy/SiC_p composite foams, SiC particles are observed in the Mg alloy/10-SiC_p composite foam with a porosity of 80.8% and the Mg alloy/80-SiC_p composite foam with a porosity of 81.2%, as shown in Figs. 1(c) and 1(e), respectively. Both the Mg alloy foam and the Mg alloy/SiC_p composite foams have a closed cell structure and exhibit a uniform cell distribution with sizes of approximately 0.6–0.8 mm. The SiC particles have no obvious influence on the cell structure of Mg alloy/SiC_p composite foams. Furthermore, heterogeneities and morphological defects such as uneven cell-wall thickness (arrows A_1, A_2, and A_3), fractured/missing cell walls (arrows B_1, B_2, and B_3), and cell-wall buckling (arrows C_1, C_2, and C_3) are observed in the cell structure. We predict that these defects may serve as internal friction sources to dissipate energy when the composite foams are subjected to a circular force in the damping tests. Figs. 1(c) and 1(e) show the SEM micro-

graphs of the SiC particles in Mg alloy/SiC_p composite foams. The SiC particles are uniformly distributed inside the cell wall or the plateau boundary of Mg alloy/SiC_p composite foams, without agglomeration. The SiC particles (arrows D_1 and D_2) are also embedded into the Mg matrix, and the interface between them is distinct.

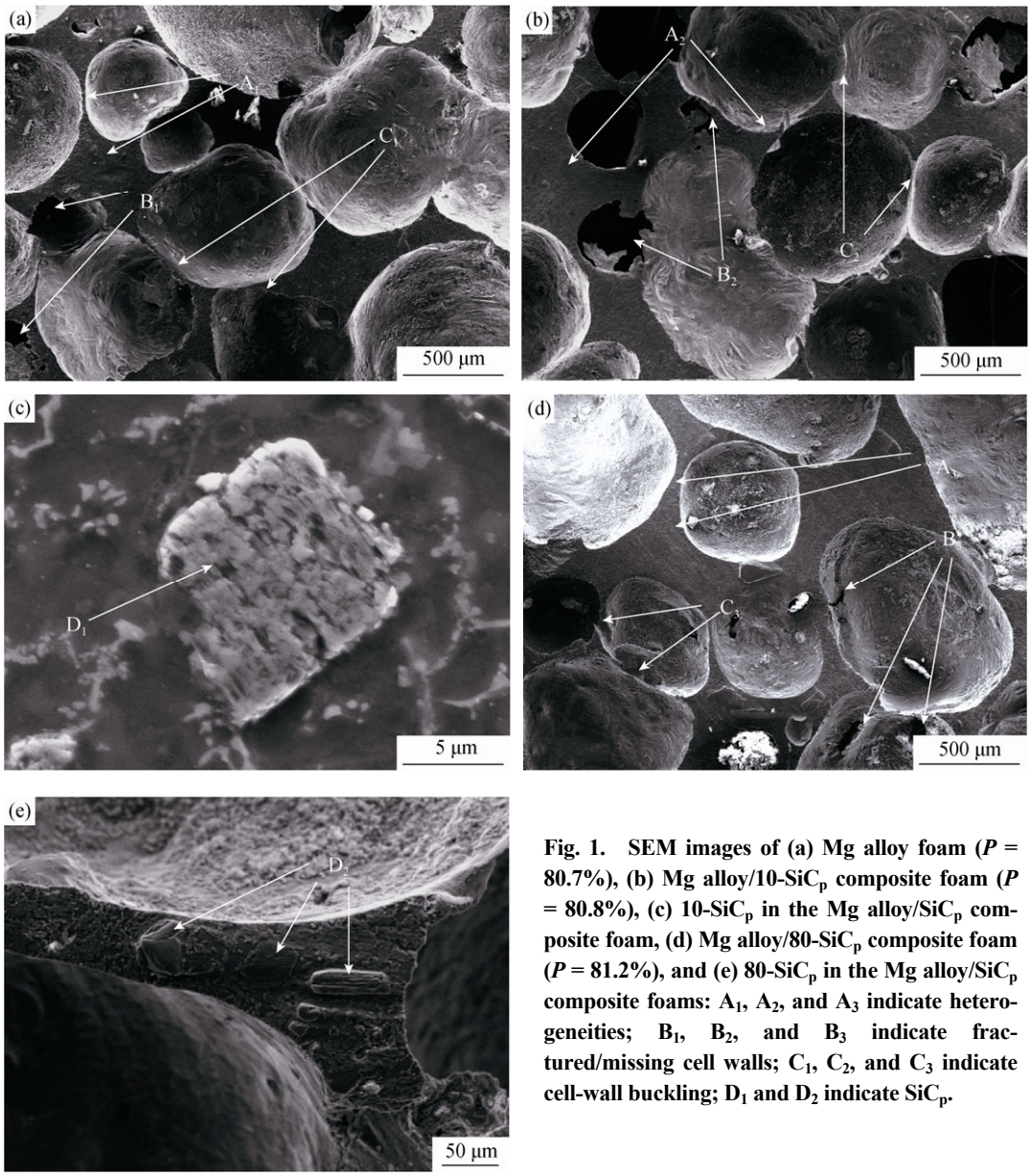

Fig. 1. SEM images of (a) Mg alloy foam (P = 80.7%), (b) Mg alloy/10-SiC_p composite foam (P = 80.8%), (c) 10-SiC_p in the Mg alloy/SiC_p composite foam, (d) Mg alloy/80-SiC_p composite foam (P = 81.2%), and (e) 80-SiC_p in the Mg alloy/SiC_p composite foams: A_1, A_2, and A_3 indicate heterogeneities; B_1, B_2, and B_3 indicate fractured/missing cell walls; C_1, C_2, and C_3 indicate cell-wall buckling; D_1 and D_2 indicate SiC_p.

3.2. Damping properties

The temperature dependence of the damping capacities of the Mg alloy foam and the Mg alloy/SiC_p composite foams are shown in Fig. 2. The specimens were heated from 40 to 400°C; the measurement frequency and amplitude were 0.5 Hz and 5 μm, respectively. A critical temperature T_{crit} was observed for each specimen. When the temperature is less than T_{crit}, the curve for each specimen is nearly horizontal and the loss factor is independent of the temperature. However, the loss factor increases remarkably when the temperature exceeds T_{crit}. In the case of the Mg alloy/SiC_p composite foams, the T_{crit} values are nearly identical, with values of approximately 250°C. By contrast, the T_{crit} value of the Mg alloy foam is lower and approximately 200°C, indicating that the T_{crit} value of the Mg alloy foam increases with the addition of SiC particles. Compared to the damping properties of Mg alloys reported in the literature [17–19], the loss factors of the Mg alloy composite foams fluctuated. The damping behaviors of both the Mg alloy foam and its com-

posite foams embody not only the characteristics of the matrix material but also their own unique property.

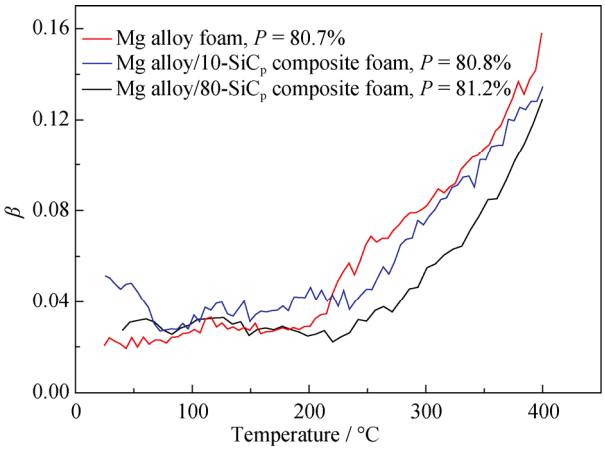

Fig. 2. Temperature-dependent loss factor β of the Mg alloy foam, Mg alloy/10-SiC_p and Mg alloy/80-SiC_p composite foams under the conditions of a frequency of 0.5 Hz and an amplitude of 5 μm.

Fig. 3 shows the high-temperature damping capacity of the Mg alloy foam and the Mg alloy/10-SiC_p and Mg alloy/80-SiC_P composite foams at different frequencies (0.5, 2.0, and 5.0 Hz). These results indicate that the Mg alloy foam and its composite foams are all frequency independent when the temperature is less than T_{crit}. However, when the temperature exceeds T_{crit}, the loss factor becomes sensitive to frequency and increases with decreasing frequency. The effect of frequency on the high-temperature damping capacity of Mg alloy composite foams is similar to that of the Mg alloy and its composites [2,12,20]. Fig. 4 shows the typical curve of the loss factor β of the Mg alloy/80-SiC_p composite foam varying with frequency. Because the test was conducted at room temperature, the frequency only slightly affects the damping capacity in the investigated frequency range. These results are in good agreement with the frequency independence at low temperatures in Fig. 3.

3.3. Effect of SiC_p on the high-temperature damping capacity

As illustrated in Fig. 2, the damping capacities of the Mg alloy/SiC_p composite foams are higher than that of the Mg alloy foam and the Mg alloy/10-SiC_p composite foam exhibits the highest damping capacity among the investigated foams in the temperature range from 40 to 200°C. Because the loss factors of the Mg alloy foam and its composite foams reflect the characteristics of the matrix material, the improved damping capacities of the Mg alloy/SiC_p composite foams mainly result from SiC particles and their modification of the microstructure of the Mg alloy matrix. The modified microstructure mainly includes the grain size, microplastic deformation of the particles, thermal-mismatch-induced dislocations, and the interfaces between SiC particles and the Mg matrix [2,9]. Moreover, the improvement of damping capacity is also attributed to the increasing interfacial microslip and microplasticity deformation arising from microcracks at the Mg alloy–SiC_p interfaces [21]. For the same amount of SiC_p added in the two Mg alloy/SiC_p composite foams, 10-μm SiC particles outnumbered 80-μm SiC particles. Thus, on the basis of the previous discussion, the Mg alloy/10-SiC_p composite foam

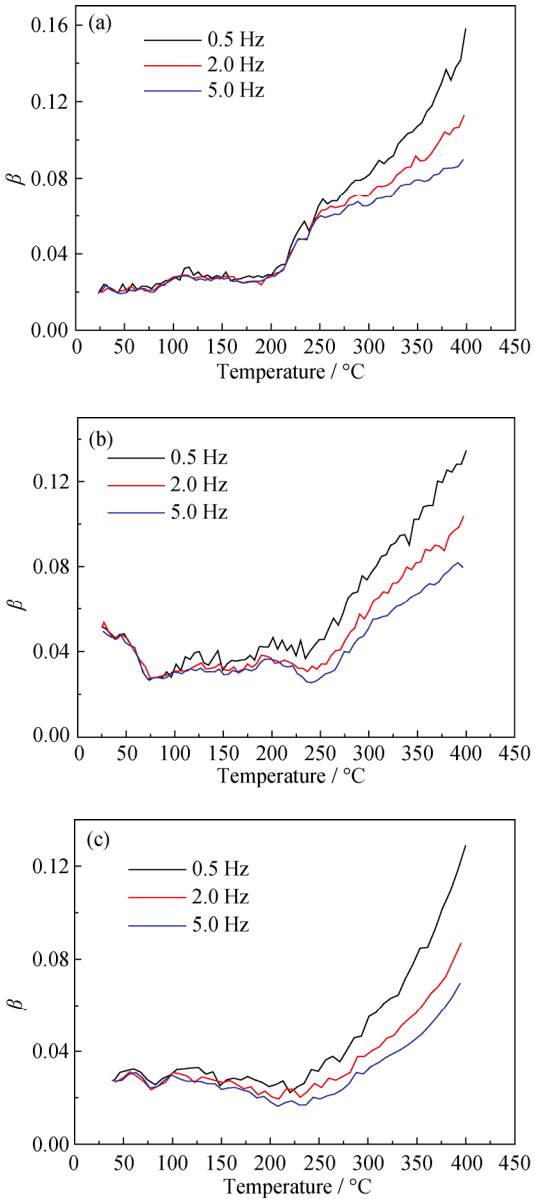

Fig. 3. Temperature dependence of loss factor β at various frequencies: (a) Mg alloy foam; (b) Mg alloy/10-SiC_p composite foam; (c) Mg alloy/80-SiC_p composite foam.

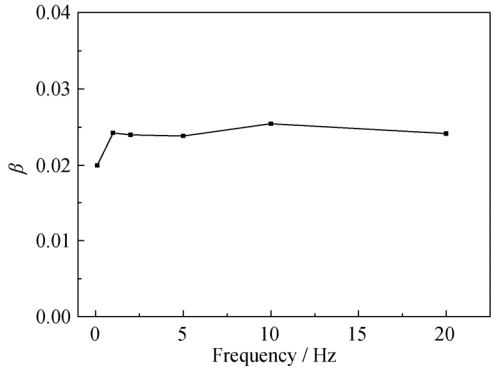

Fig. 4. Loss factor β of the Mg alloy/80-SiC$_p$ composite foam versus frequency with an amplitude of 5 μm at room temperature.

exhibits the best damping capacity. Ceramic particles were reported to exert the same effect on ZA22 alloy and Al composite foams [9,21]. However, micron and submicron SiC particles have the opposite effect on the AZ91 composite alloy. Because the submicron SiC particles contain fewer surface defects than the micron-scale SiC particles, the interfacial bonding of Mg/submicron SiC$_p$ is better than that of Mg/micron SiC$_p$ [2].

Notably, the Mg alloy foam exhibits the best damping capacity at measurement temperatures greater than 250°C, as shown in Fig. 2. This result is mainly attributed to macrodefects in the cell walls, which lead to much greater energy dissipation during loading. In the damping tests, microslip and microplasticity deformation occurred at macrodefects much more easily than at other locations in the wall. Because the yield stress of the Mg/SiC$_p$ alloy composite foams is enhanced with the addition of SiC particles, microslip and microplasticity deformations are more prone to occur in the macrodefects of the Mg alloy foam when the measurement temperature exceeds T_{crit}. Specifically, the Mg/SiC$_p$ alloy composite foams contained substantially fewer macrodefects than the Mg alloy foam, which resulted in a better damping capacity for the Mg alloy foam at high temperatures and at a lower T_{crit}; the T_{crit} value of the Mg alloy foam was 200°C, whereas that of the Mg alloy/SiC$_p$ composite foams was 250°C.

In general, the number of interfaces plays a major role in determining the damping behavior of the Mg alloy composite foams at low temperatures. The effective macrodefects in the Mg alloy composite foams caused by the added SiC particles play a major role at high temperatures.

3.4. Deformation type of macrodefects at high temperatures

Macrodefects such as fractured/missing cell walls and cell wall buckling can be observed in Figs. 1(a), 1(b), and 1(d). In fact, these defects are the internal friction source for metal foam to dissipate energy [6,22]. Thus, several modes are suggested to describe the deformation mechanism of macrodefects as internal friction sources, including cracks, a lack of defects, and weak links, as shown in Fig. 5. In Fig. 5(a), the component of stress F in the direction of F_1 or F_1' is an effective and easily induced internal friction source. However, the component in the direction of F_2 or F_2' is hard to slide and does not affect the energy dissipation. In Fig. 5(b), the components of stress F in the directions of both F_1 or F_1' and F_2 or F_2' are all effective stress and can become the internal friction source. In Fig. 5(c), the component in the direction of F_1 or F_1' is prone to induce cell-wall buckling, which can become an internal friction source, whereas that in the direction of F_2 or F_2' cannot easily become effective stress. By contrast, it can also become an internal friction source to dissipate energy when a strong heterogeneity in stress distribution occurs.

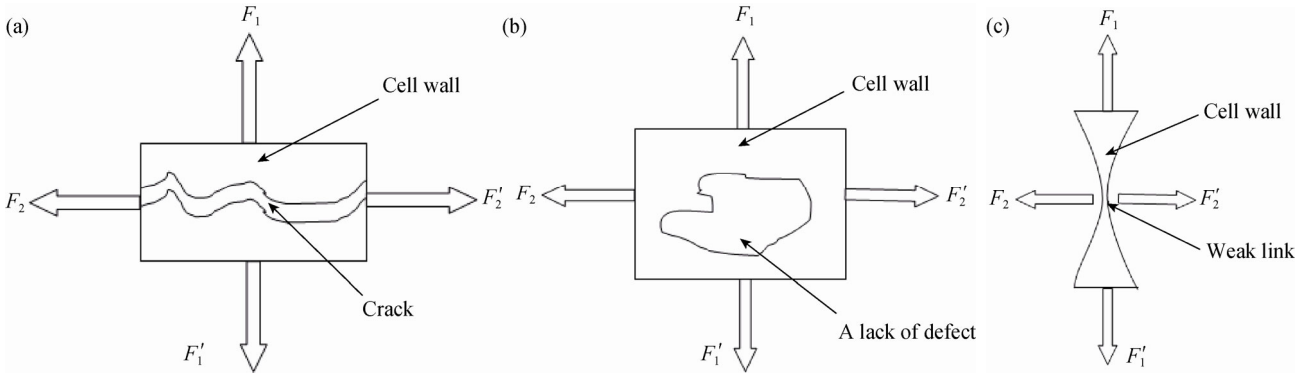

Fig. 5. Different types of macrodefects: (a) cracks; (b) a lack of defects; (c) weak links.

As discussed previously, both the cellular structures and the matrix material have evident effects on the damping properties of the Mg alloy foam and its composite foams. An equation can be constructed as follows:

$$E = E_{I1} + E_{I2} + E_{I3} + E_{WL} + E_{LD} + E_C \quad (3)$$

where E is the energy dissipation of Mg alloy/SiC_p composite foams in the damping tests; E_{I1} and E_{I2} are the energy dissipation caused by the movement of dislocations and the sliding of grain boundaries, respectively; E_{I3} is the energy dissipation caused by SiC particles; and E_{WL}, E_{LD}, and E_C are the energy dissipation caused by weak links, a lack of defects, and cracks in the cell structure of the Mg alloy/SiC_p composite foams, respectively. Parameters E_{I1}, E_{I2}, and E_{I3} are attributed to the properties of the matrix material, i.e., Mg alloy/SiC_p composites; E_{WL}, E_{LD}, and E_C are caused by macrodefects in the cell structure of Mg alloy/SiC_p composite foams.

In this work, when the temperature is less than T_{crit}, energy dissipation caused by the characteristics of the matrix material ($E_{I1} + E_{I2}$) and macrodefects ($E_{WL} + E_{LD} + E_C$) is lasting, and E_{I3} plays a major role in energy dissipation. In turn, macrodefects ($E_{WL} + E_{LD} + E_C$) play a major role when the temperature exceeds T_{crit}.

4. Conclusions

(1) The Mg alloy composite foams were fabricated via a melt foaming route using $MgCO_3$ as the blowing agent.

(2) The loss factor of the Mg alloy foam and its composite foams is insensitive to temperature and loading frequency when the temperature is less than the critical temperature T_{crit} but increases remarkably with increasing temperature when the temperature exceeds T_{crit}. The T_{crit} values for the Mg alloy foam and the Mg alloy/SiC_p composite foams are 200 and 250°C, respectively.

(3) The Mg alloy/10-SiC_p composite foam exhibits the highest damping capacity when the temperature is below 200°C. However, the Mg alloy foam exhibits the best damping capacity when the measurement temperature exceeds 250°C. This difference is attributed to the changes in the characteristics of the matrix material, to abundant interfaces and interfacial slipping caused by SiC particles, and to macrodefects in the Mg alloy composite foam.

(4) The damping properties of the Mg alloy foam and its composite foams are determined by both cellular structures and the matrix material. The equation $E = E_{I1} + E_{I2} + E_{I3} + E_{WL} + E_{LD} + E_C$ was constructed for the damping mechanism. Different internal friction sources play major roles at different temperatures.

Acknowledgments

This work was financially supported by the National Natural Science Foundation of China (Nos. 51174060 and 51301109), the Science and Technology Department of Liaoning Province of China (No. 2013223004), and the Fundamental Research Funds for the Central Universities (No. 140203004).

References

[1] J.H. Gu, X.N. Zhang, Y.F. Qiu, and M.Y. Gu, Damping behaviors of magnesium matrix composites reinforced with Cu-coated and uncoated SiC particulates, *Compos. Sci. Technol.*, 65(2005), No. 11-12, p. 1736.

[2] K.K. Deng, J.C. Li, K.B. Nie, X.J. Wang, and J.F. Fan, High temperature damping behavior of as-deformed Mg matrix influenced by micron and submicron SiC_p, *Mater. Sci. Eng. A*, 624(2015), p. 62.

[3] X.H. Liu, H.Y. Huang, and J.X. Xie, Effect of strain rate on the compressive deformation behaviors of lotus-type porous copper, *Int. J. Miner. Metall. Mater.*, 21(2014), No. 7, p. 687.

[4] D.R. Tian, Y.H. Pang, L. Yu, and L. Sun, Production and characterization of high porosity porous Fe–Cr–C alloys by the space holder leaching technique, *Int. J. Miner. Metall. Mater.*, 23(2016), No. 7, p. 793.

[5] C.S. Liu, Z.G. Zhu, F.S. Han, and J. Banhart, Internal friction of foamed aluminium in the range of acoustic frequencies, *J. Mater. Sci.*, 33(1998), No. 7, p. 1769.

[6] F.S. Han, Z.G. Zhu, C.Y. Shi, and Y. Wang, Study on the damping characteristics of foamed aluminum, *Acta Phys. Sin.*, 47(1998), No. 7, p. 1161.

[7] J. Banhart, J. Baumeister, and M. Weber, Damping properties of aluminium foams, *Mater. Sci. Eng. A*, 205(1996), No. 1-2, p. 221.

[8] J.N. Wei, C.L. Gong, H.F. Cheng, Z.C. Zhou, Z.B. Li, J.P. Shui, and F.S. Han, Low-frequency damping behavior of foamed commercially pure aluminum, *Mater. Sci. Eng. A*, 332(2002), No. 1-2, p. 375.

[9] J.J Wu, C.G Li, D.B Wang, and M.C Gui, Damping and sound absorption properties of particle reinforced Al matrix composite foams, *Compos. Sci. Technol.*, 63(2003), No. 3-4, p. 569.

[10] M.C. Gui, D.B. Wang, J.J. Wu, G.J. Yuan, and C.G. Li, Deformation and damping behaviors of foamed Al–Si–SiC_p composite, *Mater. Sci. Eng. A*, 286(2000), No. 2, p. 282.

[11] Y.L. Mu, G.C. Yao, and H.J. Luo, The dependence of damping property of fly ash reinforced closed-cell aluminum alloy foams on strain amplitude, *Mater. Des.*, 31(2010), No. 2, p. 1007.

[12] N. Ma, Q.M. Peng, J.L. Pan, H. Li, and W.L. Xiao, Effect of microalloying with rare-earth on recrystallization behaviour and damping properties of Mg sheets, *J. Alloys Compd.*, 592(2014), p. 24.

[13] D.H. Yang, S.R. Yang, H. Wang, A.B. Ma, J.H. Jiang, J.Q.

Chen, and D.L. Wang, Compressive properties of cellular Mg foams fabricated by melt-foaming method, *Mater. Sci. Eng. A*, 527(2010), No. 21-22, p. 5405.

[14] L. Chen, C.L. Liu, Q.M. Zhang, Z.G. Xu, and Y.S. Yang, Mechanical properties and energy absorption characteristic of magnesium foam under static and dynamic compression, *Acta Armamentarii*, 30(2009), Suppl. 2, p. 197.

[15] Z.G. Xu, J.W. Fu, T.J. Luo, and Y.S. Yang, Effects of cell size on quasi-static compressive properties of Mg alloy foams, *Mater. Des.*, 34(2012), p. 40.

[16] Y. Yamada, K. Shimojima, Y. Sakaguchi, M. Mabuchi, M. Nakamura, T. Asahina, T. Mukai, H. Kanahashi, and K. Higashi, Effects of heat treatment on compressive properties of AZ91 Mg and SG91A Al foams with open-cell structure, *Mater. Sci. Eng. A*, 280(2000), No. 1, p. 225.

[17] X.S. Hu, K. Wu, M.Y. Zheng, W.M. Gan, and X.J. Wang, Low frequency damping capacities and mechanical properties of Mg–Si alloys, *Mater. Sci. Eng. A*, 452-453(2007), p. 374.

[18] X.S. Hu, Y.K. Zhang, M.Y. Zheng, and K. Wu, A study of damping capacities in pure Mg and Mg–Ni alloys, *Scripta Mater.*, 52(2005), No. 11, p. 1141.

[19] X.S. Hu, X.D. He, M.Y. Zheng, and K. Wu, Effect of small tensile deformation on damping capacities of Mg–1%Al alloy, *Trans. Nonferrous Met. Soc. China*, 20(2010), Suppl. 2, p. s444.

[20] Y.W. Wu, K.Wu, K.K. Deng, K.B. Nie, X.J. Wang, X.S. Hu, and M.Y. Zheng, Damping capacities and tensile properties of magnesium matrix composites reinforced by graphite particles, *Mater. Sci. Eng. A*, 527(2010), No. 26, p. 6816.

[21] Y.L. Mu, G.C. Yao, G.Y. Zu, and Z.K. Cao, Influence of strain amplitude on damping property of aluminum foams reinforced with copper-coated carbon fibers, *Mater. Des.*, 31(2010), No. 9, p. 4423.

[22] I.S. Golovin and H.R. Sinning, Damping in some cellular metallic materials, *J. Alloys Compd.*, 355(2003), No. 1-2, p. 2.